JOURNAL OF OPTOELECTRONICS AND ADVANCED MATERIALS, Vol. 10, No. 9, September 2008, p. 2470 - 2473

Simulation of nanoparticle formation by condensation from the gaseous phase

I. NICOLAE, M. POPESCU[a]
National Institute R&D for Laser, Plasma and Radiation Physics, P. O. Box MG. 6, 77125-Bucharest-Magurele, Romania
[a]National Institute R&D of Materials Physics, P.O. Box MG. 7, 77125-Bucharest-Magurele, Romania

The paper reports the computer simulation of nanoparticle formation based on classical homogenous condensation theory with the purpose of understanding nanoparticle formation and the dependence of their size distribution on process parameters. The simulation has been performed for the case of silicon. The process of condensation with the formation of clusters due to the high cooling speed (~10^4-10^5 K/s) is considered.

(Received July 25, 2008; accepted August 14, 2008)

Keywords: Nanoparticle, Size distribution, Silicon, Simulation, Clusters

1. Introduction

The integration of devices to very large scale comes to the limit of the material [1]. Thus, the investigation of the particle formation and properties at the nanoscale of the particular solid state material is a subject of great interest nowadays. Nanocrystalline materials for hydrogen storage were developed [2]. Nanosized magnetite particles are useful for medicine [3]. Organic LED can be activated by nanocrystalline quantum dots [4]. The nano-crystallinbe iron based alloys shows unusual properties [5]. Generation of oxide nanoparticles via femtosecond laser ablation has been performed [6]. The modeling of the nano-structural disorder in hydrogenated amorphous silicon was carried out [7]. Germanium nano-dots were obtained during sol-gel deposition [8]. The synthesis of nano-crystalline tin oxide powder was achieved by M. Pal Singh et al. [9]. Polymer microspheres for drug delivery have been prepared [10]. Mixed SnS_2 and TiO_2 powdered catalysts were synthesized by wet chemical methods and exhibited high efficiency in the solar-assisted decomposition of organic compounds [11].

Nanoparticle production is a field of particular interest due to physical challenges and multiple practical applications. Since the production of large quantities of nanoparticles with desired qualities and low dispersion requires a thorough understanding of the formation process, much research effort has been made to that direction. It has been experimentally determined that any process of evaporation of high vaporization point materials followed by condensation at room temperature results in nanoparticle formation [12,13].

Our aim is to determine what process characteristics are needed in order to lead to nanoparticle formation. We have tried to solve that problem by simulating the condensation process of the silicon vapors, and adjusting the process parameters until the resulting particle dimensions were in the nanometer range.

2. Theory

We have simulated the silicon nanoparticle formation in the framework of the classical homogenous condensation theory, with the following approximations: neglecting of the sub-molecular regime, constant pressure, constant cooling speed, constant number of atoms per condensation nuclei, unitary growth coefficient.

The signification of the symbols used in this paper is as follows: p – Si vapor pressure, V_T – cooling speed, dt – time incremental step, m_o – Si atomic mass, v_o – Si atomic volume, σ – Si superficial tension [14], α – growth coefficient.

The condensation nuclei formation rate is given by [15]:

$$J(T,p)=\sqrt{\frac{2\sigma}{\pi m_o}}\frac{v_o p p_\infty(T)}{kT^2}e^{-\frac{16\pi v_o^2\sigma^3}{3(kT)^3}} \quad (1)$$

where $p_\infty(T)$ is the Si vapor pressure at temperature T. $p_\infty(T)$ is given by [16]:

$$p_\infty(T)=e^{\frac{A}{T}+B} \quad (2)$$

where the coefficients A and B were determined by fitting the experimentally determined values for Si vapor pressure [17].

The silicon vapors are considered as forming an under-cooled assembly, and, therefore, we admit that all the atoms colliding with a Si cluster are condensing, the growth process being described by [18]

$$I(T,p)=\frac{\alpha}{\sqrt{2\pi m_o kT}}(p-p_\infty(T)) \quad (3)$$

where I(T, p) is the evaporation/condensation rate per surface unit per second. The growth process takes place only if $p > p_\infty(T)$.

A special computer program was developed. The algorithm is schematically represented in Fig. 1:

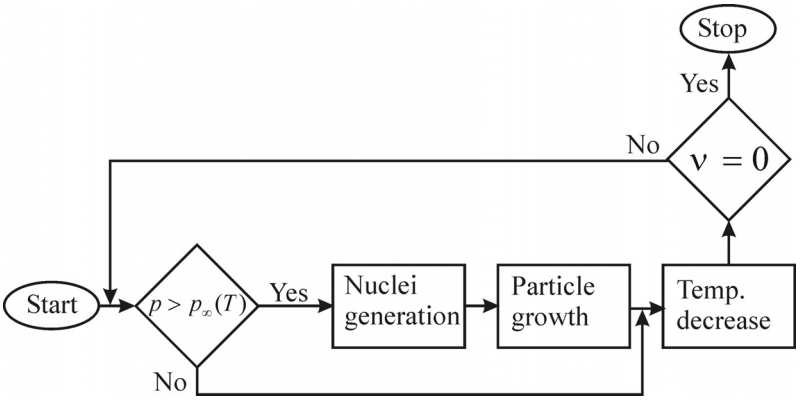

Fig. 1. Logical scheme of the algorithm.

The simulation algorithm steps are as follows:

a) The initial conditions and parameter of simulation are set up: quantity of ν moles of silicon vapor, initial temperature T_o and pressure p, cooling speed V_T (in degrees per second), and time increment dt.

b) The condition $p > p_\infty(T)$ is tested. If true, the program continues with step c); if false, the program jumps to step e).

c) A number of nuclei are generated, according to temperature T and pressure p (modeled by eq. 1).

d) A number of atoms are condensing on existing nanoparticles, according to temperature T and pressure p (modeled by eq. 3).

e) The temperature T is decreased with $V_T dt$.

f) The condition ν=0 is tested. If true, the program continues with step g); if false, the program jumps to step b).

g) Stop.

3. Results

By running the simulation program for various cooling speeds and pressures, the following results have been obtained:

- The size-distribution resulting from the simulation have a close resemblance with a lognormal distribution, which fits it well (Fig. 2).
- The size-distribution of the nanoparticles exhibits a close resemblance with the size-distributions determined experimentally [12,13].
- The peaks of the distributions shift toward smaller radiuses and become narrower with the increase of the cooling speed (Fig. 4).

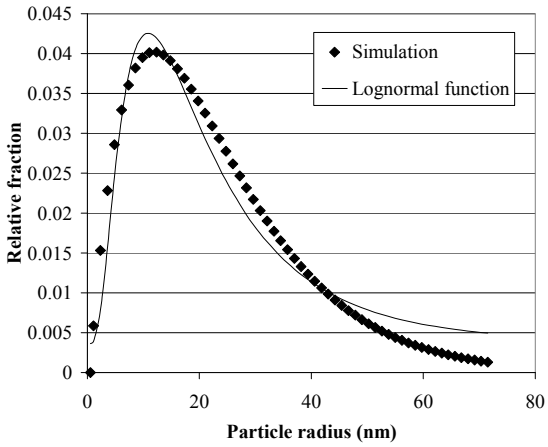

Fig. 2 Simulated nanoparticle size-distribution fit with a lognormal function. The simulation was made for p=70 kPa and V_T=70 000 K/s.

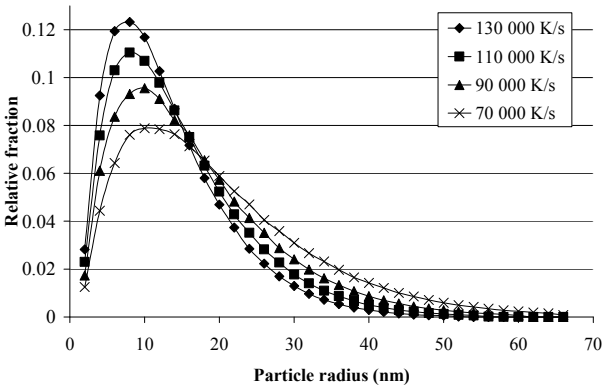

Fig. 4 Nanoparticle size-distributions for various cooling speeds. All simulations were made at p=50 kPa.

- A similar behaviour was noticed with the decrease of pressure (Fig. 5).

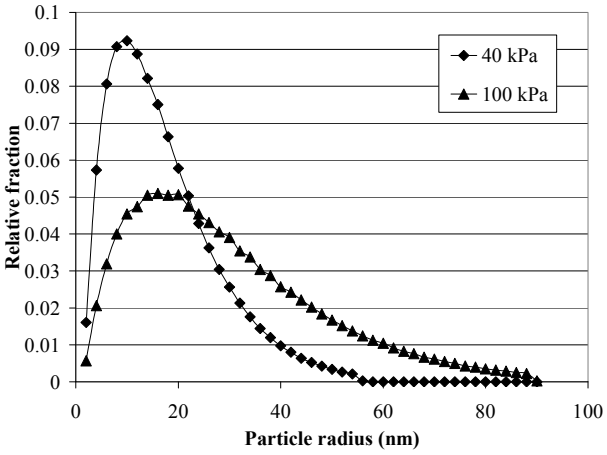

Fig. 5. Nanoparticle size-distributions for two pressures. Both simulations were made at V_T=70 000 K/s.

4. Discussion

While the pressure and temperature determines the rate formation (the nuclei per unit volume), the number of condensed nuclei depends on the available material as well. Because the nuclei formation and particles growth are concurrent and competing processes (they both consume the vapors), one can conclude that the process parameters that lead to nanoparticle formation must maximize the nuclei formation rate relative to the particle growth rate.

From figure 6 one observes that the increase of the condensation nuclei formation rate with temperature decrease is much steeper than the increase of the particle growth rate. The consequence of this behaviour is that as the temperature decreases, the nuclei generation process is increased with a higher rate than the particle growth, so a faster cooling speed will result in a higher number of particles. Given a fixed quantity of Si vapors, it is obvious that the higher the number of particles resulting from condensation, the smaller their mean dimension will be, thus explaining the observed nanoparticle size-distribution dependence of the cooling speed.

Experiment [6] shows that nanoparticle size distribution of several metallic oxides (NiO, ZnO, CuO) and average size can be directly controlled by laser fluences and pulse numbers. Thus, if the oxide target is irradiated by femtosecond laser pulses, the ablated particle sizes are in the range of 76 – 93 nm, raising from the bottom value for 10 laser pulses up to the top value for 500 laser pulses. These values are higher than those obtained for silicon. In the case of nickel oxide particles the average size for 10 laser pulses is 50 nm, a value that is more approached to the mean size obtained for silicon (both experiment and simulation).

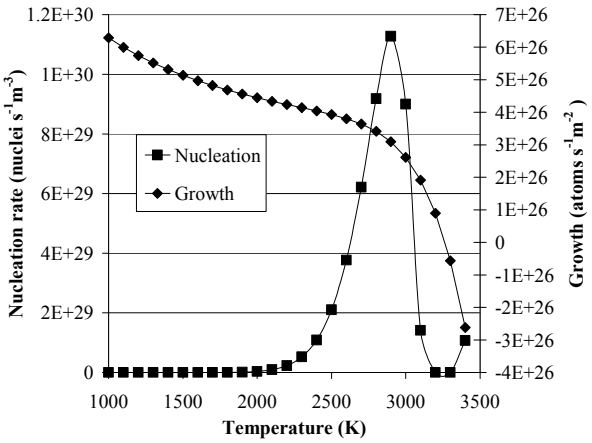

Fig. 6. Nucleation rate and growth rate as a function of temperature. The values are given for p=40 kPa.

Fig. 7 illustrates the growth rate at different pressures as a function of temperature. It can be seen that the growth rate decreases with the decrease of pressure. Thus, the nanoparticle size-distribution shift toward smaller dimensions is explained by the fact that the growth process is reduced by the pressure decrease.

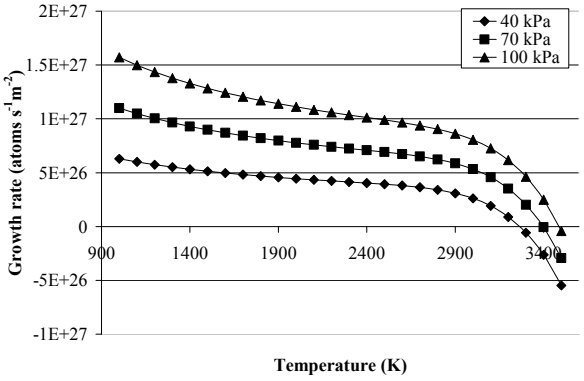

Fig. 7. Growth rate at various pressures.

The modifications of average size of the particles induced by heat and pressure is accompanied by important variation of the defects generated into particles. High-resolution electron microscopy studies of metal nanoparticles evidence shape and twin defects, as well as surface stress effects [19]. These defects could determine a further breaking of the nanoparticles and formation of smaller size ones.

5. Conclusions

The above described simplified model, proposed for nanoparticle formation, can successfully explain the nanoparticle formation and their size-distribution.

The modification of the nanoparticle size-distribution

with the process parameters is due to the role played by these parameters in the two competing processes: nuclei formation and particle growth. When the nuclei formation is favored the particle growth is reduced.

References

[1] M. Popescu, J. Optoelectron. Adv. Mater. **8**(2), 755 (2006).
[2] M. Jurczyk, J. Optoelectron. Adv. Mater. **8**(2), 418 (2006).
[3] I. Nedkov, J. Optoelectron. Adv. Mater. **9**(1), 24 (2007).
[4] K. Kohary, V. M. Butlakov, D. G. Pettifor, J. Optoelectron. Adv. Mater. **9**(1), 18 (2007).
[5] E. Burzo, C. Djega-Mariadassou, J. Optoelectron. Adv. Mater. **9**(6), 1757 (2007).
[6] Sun Qi, Ni Xiaochang, Li Haiyan, Wang-Ching-yue, Chai Lu, Yang Li, Jia Wei, J. Optoelectron. Adv. Mater. **9**(7), 2162 (2007).
[7] F. Sava, J. Optoelectron. Adv. Mater. **9**(9), 2963 (2007).
[8] T. F. Stoica, M. Gartner, V. S. Teodorescu, T. Stoica, J. Optoelectron. Adv. Mater. **9**(10), 3271 (2007).
[9] Manmeet Pal Singh, P. Singh Chandi, R. C. Singh, J. Optoelectron. Adv. Mater. **9**(10), 3275 (2007).
[10] K. Ulubayram, Y. Tunc, E. Baykara, J. Optoelectron. Adv. Mater. **9**(11), 3479 (2007).
[11] H. Y. He, J. F. Huang, L. Y. Cao, J. P. Wu, Z. He, L. Luo, J. Optoelectron. Adv. Mater. **9**(12), 3781 (2007).
[12] S. Amoruso, G. Ausanio, R. Bruzzese, M. Vitiello, X. Wang, Femtosecond laser pulse irradiation of solid targets as a general route to nanoparticle formation in a vacuum, Phys. Rev. B vol. **71**, p. 033406 (2005).
[13] W. Marine, L. Patrone, B. Luk'yanchuk, M. Sentis, Strategy of nanocluster and nanostructure synthesis by conventional pulsed laser ablation, Apl. Surf. Sci., **154-155**, 345, (2000).
[14] H. Fujii, T. Matsumoto, S. Izutani, S. Kiguchi, K. Nogi, Surface tension of molten silicon measured by microgravity oscilating drop method and improved sessile drop method, Acta Materialia **54**(5), 1221 (2006).
[15] D. W. Oxtoby, J. Phys.: Condens. Matter Homogenous nucleation: theory and experiment **4**, 7627 (1992).
[16] Vapor-pressure data extrapolated to 1000 atmospheres (1.01~108 N/m^2) for 13 refractory materials with low thermal absorption cross sections, C. C. Maser, Nasa TN D-4147, National Aeronautics and Space Administration, (1967).
[17] P. D. Desai, Thermodynamic properties of iron and silicon, J. Phys. Chem. Ref. Data **15**(3), (1986).
[18] R. F. Strickland-Constable, Kinetics and Mechanism of Crystallization, Academic Press, 1968.
[19] H. Hofmeister, J. Optoelectron. Adv. Materials **9**(1), 99 (2007).

*Corresponding author: ionut@nipne.ro